THE NUMERICAL ANALYSIS OF A PZL-106 KRUK WING SLAT TOLERANCE FOR A BIRD STRIKE DAMAGE

Adam Deskiewicz
Warsaw University of Technology,
Faculty of Power and Aeronautical Engineering
ul. Nowowiejska 24
00-665 Warszawa, Poland
adeskiewicz@meil.pw.edu.pl

Rafał Perz
Warsaw University of Technology,
Faculty of Power and Aeronautical Engineering
ul. Nowowiejska 24
00-665 Warszawa, Poland
rperz@meil.pw.edu.pl

Abstract. Collisions of aircraft and airborne objects are inevitable in aviation. Birds are unalterably among the major threats to aircraft in low level flight. Possible consequences of a bird strike have been analysed and described in this paper. A fixed slat segment of a Polish designed PZL-106 Kruk aircraft wing has been chosen for analysis. It is particularly susceptible to bird strikes due to its placement on the wing's leading edge as well as the agricultural utility of the aircraft of interest. The finite element model of the analysed part has been created. Bird models of various weight have been tested according to the framework found in aeronautical certification standards. Smooth Particle Hydrodynamics (SPH) formulation has been used for generation of the bird finite element model. The simulations were performed by the LS Dyna explicit finite element analysis software. Used methods have been validated by performing a sample simulation and subsequent comparison of obtained results with the experimental data available in literature. A number of test cases have been analysed which differed in parameters such as impact velocity, initial velocity vector direction, place of impact and bird mass. The results have been presented and potential influence of the deformed slat on the remaining parts of the wing has been discussed. Subsequently, loads acting on slat fixings during the bird strike have been analysed and the possibility of slat segment detachment from the wing has been examined. The simulation outcome gives the manufacturer a better insight into the behaviour of this particular aircraft part in case of a bird strike without carrying out expensive tests using real aircraft components.

Keywords. Bird strike, Explicit Finite Element Method, Impact analysis

1 Introduction

Birds have posed a threat to aviation ever since Wright brothers hit a bird by their Flyer III in 1905 [1]. A recent accident of an Airbus A320 with 155 people onboard forced to perform an emergency landing on the Hudson River near the New York City, USA [2] indicates that the problem is still unsolved. The reason were multiple bird impacts that consequently led to both engines shutdown.

Despite the attempts of prevention, such as installation of lights and shiny objects near airfields, training dogs and birds of prey, and even deployment of chemical substances intended to repel unwelcome animals [3] the danger can not be eliminated. For this reason, considering a bird strike in the design phase of each flying vehicle is inevitable. Moreover, according to previous studies [4] up to 74% of bird strikes occur at altitudes below 200 ft (60 m). It suggests, that this threat should be of particular interest in the design of agricultural aircraft, which are especially likely to hit a bird given that they fly at altitude of 15 m or lower.

Figure 1: Airbus A320 after ditching on the Hudson River. *Source: The New York Times* [2]

This simulation focuses on the damage done to the aircraft part, rather than a bird. Therefore, the complex and heterogeneous animal body needs a simplified model. A number of various methods of modelling a bird were proposed in literature. Shmotin [5] in his study applied the Lagrangian formulation, where a bond between a mesh and material exists, which effectively means that a single element cell stays with the same material through the whole simulation, which is a desired feature in case of solid elements. Even though this method allows to track element parameters changing with time, very high deformations that are inevitable in this kind of simulation may introduce errors or even lead to abnormal termination of the calculations. Poola [6] modelled a bird with the Eulerian formulation, which is more appropriate when modelling a fluid, as the mesh is fixed in space with concurrent convection of material through the elements. This formulation is, however, very expensive computationally and it is also difficult to track material interfaces and history of material parameters. Nagaraj [7] used a formulation which is effectively the combination of both aforementioned formulations. The Arbitrary Lagrangian-Eulerian (ALE) method performs an automatic rezoning when a mesh distorts. Both meshes are apparently present, the reference and material mesh. Moreover, each element may contain more than one material which in our case enables to model pressurized air surrounding the bird. Smooth Particle Hydrodynamics (SPH) formulation was applied by Guida [8]. It is grid-free and solves the issue of large deformations. SPH particles exert an attraction force on each other of the magnitude depending on the distance between them, called the soothing length. Sorting is also introduced which enables to decrease the CPU time required to calculate the distance between smooth particles by dividing the domain into small boxes in which groups of neighbouring particles interacting with each other are enclosed [9]. SPH formulation has been used in this thesis, since it is not only most commonly used in similar analyses but also it is relatively simple to implement. Using a fluid representation of a bird body may seem naive, yet a bird strike happening at relative velocities close to 100 km/h causes the body of a bird to disintegrate immediately after the crash as a portion of fluid would behave. Sufficient accuracy of this method has been proved by experiments [10] and photographs of real accidents (see Fig. 2). All aforementioned bird modelling methods were summarised by Heyadati [11].

Figure 2: Bird disintegration after a collision with an aerobatic aircraft. *Source: Daily Mail Online* [12]

Experiments on real aerospace equipment are very costly, thus a non-destructive impact damage tolerance analysis is necessary. Leading edges of lifting surfaces and lift extension devices mounted on them are among the most susceptible aircraft parts to bird strikes. Thus, a leading edge mounted slat of the PZL-106 *Kruk* agricultural aircraft has been chosen for analysis as the subject of this study. A simulation of a bird strike on the part under different conditions was performed. Subsequently, the damage caused by the bird to the component was assessed. Finally, the impact energy absorption capabilities of the fixed slat, which in the considered case is also meant to act as a shock absorber, were verified and conditions under which it does not prevent damage to the wing box were determined.

Figure 3: PZL-106 KRUK BTU-34. *Courtesy of PZL "Warszawa - Okęcie" S.A.*

2 Methods

The slat consists of 4 segments of 1598 mm width along the semi-span of the aircraft. Each segment is supported at both ends by metal fixings attached to the main part of the wing by bolts as illustrated in Figure 4. Aluminium 2024 (K-PA7) is a base material for all parts that differ in sheet thickness only. All parts included in the slat assembly are listed in Table 1.

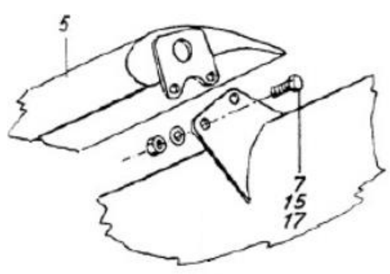

Figure 4: Slat-wing connection. *Courtesy of PZL "Warszawa - Okęcie" S.A.*

Table 1: Component list of a single slat segmen

Part name	Quantity	Metal sheet thickness [mm]
Side rib	2	1.0
Aft rib	4	0.6
Nose rib	4	0.6
Spar	1	1.0
L-profile	2	1.0
Upper skin	1	0.8
Lower skin	1	0.5
Fixing	2	2.0

Parts such as trailing edge inserts, despite being important from the manufacturing point of view, are of minor importance in this analysis and, therefore, are not listed in Table 1.

The CAD geometry as well as technical drawings of all components has been provided by the aircraft manufacturer - PZL "Warszawa – Okęcie" S.A. Provided CAD files contained the slat components in their original, currently manufactured form. All slat components were made of metal sheet and, therefore, shell elements were chosen for this analysis. From all possible shell element types available in LS Dyna a fully integrated shell type has been used in the *SECTION_SHELL keyword. A default Belytschko-Tsay shell element, which is in fact 2.5 times less expensive computationally [13] and gives reasonably accurate results, has only one in-plane integration point which enables the occurrence of hourglass modes. Hourglassing causes severe deformation of finite elements and consequently the inaccuracy of obtained results.

A spotweld connection defined by the keyword *CONSTRAINED_SPOTWELD has been applied to model rivet connections of two metal sheets. In order to model rivets which join three or more sheets the *CONSTRAINED_NODAL_RIGID_BODY keyword had to be used. Both methods effectively couple selected nodes in terms of all six degrees of freedom. No rivet failure mode has been implemented. Final mesh of the slat included 61333 shell elements, 246 spotweld connections and 66 nodal rigid bodies. The final form of the mesh is illustrated in Figures 5 and 6.

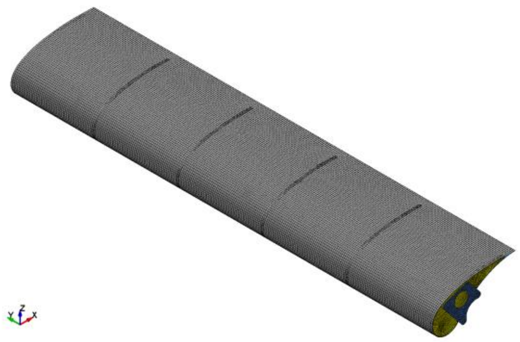

Figure 5: Mesh of the complete slat

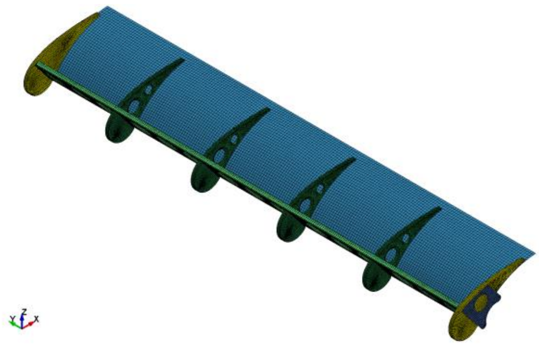

Figure 6: Slat model interior

A standard material law to describe an elastic-plastic material behaviour defined by a keyword *MAT_PIECEWISE_LINEAR_PLASTICITY has been used to model Aluminium 2024. Two regions of elastic and plastic material behaviour are distinguished for this particular model. The following material properties has been used in the analysis [14], [15]:

$Density\ \rho = 2780\ kg/m^3$
$Young's\ modulus\ E = 73.1\ GPa$
$Tangent\ modulus\ E_t = 2.0\ GPa$
$Poisson\ ratio\ \nu = 0.33$
$Yield\ stress\ s_y = 324\ MPa$
$Strain\ at\ failure\ \epsilon_b = 0.2$

Taking into account the environment in which PZL-106 *Kruk* operates (i.e. rural areas, fields) a bird species to be represented in the analysis has been chosen. According to environmental statistics [16], pheasants (weighing 1.3 to 1.8 kg) and partridges (weighing 0.3 to 0.5 kg) are among the most frequently encountered birds on the fields in Poland. Nevertheless, the range of birds living in this environment is very wide and an aircraft operating there might be as well impacted by much heavier or much lighter birds [16]. 1.8 kg as a bird mass has already been used as a reference in aeronautical regulations [17], thus this value has been chosen for analysis A mass of 0.5 kg for the second bird has been chosen to represent lighter bird species.

The bird geometry might be represented for finite element analyses in a number of ways. Some of them are rather sophisticated and consist of wings, torso and head that are characterised by different mechanical properties [18]. In this study, however, the assumption of uniform properties within the entire volume of a bird model is sufficiently accurate. A frequently encountered in literature cylindrical shape with hemispherical ends has been selected having dimensional proportion presented in Figure 7.

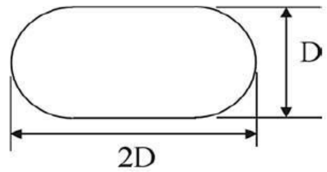

Figure 7: Proportion of the chosen bird model

Bird model dimensions were derived with the use of an experimental formula provided by the reference [19] relating the density of a bird material with its mass. The resulting bird models are:

1) $m_1 = 1.8\,kg,\ \rho_1 = 942.7\frac{kg}{m^3}, D_1 = 0.1136\,m$

2) $m_2 = 0.5\,kg,\ \rho_2 = 978\frac{kg}{m^3}, D_1 = 0.073\,m$

LS-PrePost was employed in generation of the finite element model, which consisted of 20931 SPH elements. *MAT_NULL material model has been applied complemented with an equation of state keyword. *EOS_TABULATED has been used to define the relation between state parameters of a bird particles according to the following formula:

$$p = C(\varepsilon_V) + \gamma T(\varepsilon_V)E \tag{1}$$

where T represents temperature, C is a function or a constant array, ε_V denotes natural logarithm of relative volume and E is internal energy. The second term of the equation of state may be omitted, as the temperature difference in analysed case is negligible. Therefore, the remaining part, i.e. $p = C(\varepsilon_V)$, effectively requires a number of tabulated points to be given so that the pressure values may be extrapolated. Sample values of C and ε_V found in literature [20] have been used as an input.

An initial velocity along the x axis has been applied to all elements within the model of a bird with a magnitude depending on the simulated case.

All calculations have been performed with the use of LS Dyna, a commercial explicit finite element method software. Explicit FEM is essentially an incremental method, where the current step solution is based on the previous steps only. In contrast to the implicit formulation, the stiffness matrix doesn't have to be inverted and linear change of displacement is assumed [21].

Single Point Constraint boundary condition (*BOUNDARY_SPC) has been applied to the model. Four nodes have been fixed with respect to five degrees of freedom enabling each node to rotate about y (lateral) axis simulating the operation of 4 bolts holding the structure (Fig. 8).

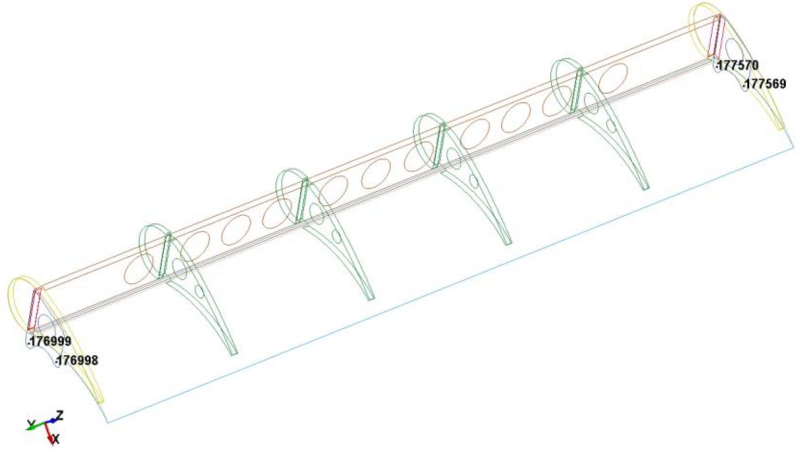

Figure 8: Boundary conditions on the slat - constrained node ID's

A termination time of 15 milliseconds has been set, so that all significant phenomena to occur in the simulation are captured. It was also limited by the duration time of a single solution which increases proportionally to the simulation termination time set.

In order to validate solution settings, used tools and applied model, a sample calculation case had been run prior to the actual study cases. In the experiment a bird weighing 1.8 kg was shot at a rectangular Al 7075 T6 plate of 0.16 inch (4.06 mm) thickness at a 90^{o} angle with the velocity of 136.33 m/s (265 knots) [20]. The comparison between the simulation outcome and the experimental data presents a very good correlation. The maximum obtained deformation was 0.0398 m (1.567 inch) which compared to 1.5 inch in experimental test suggests that methods used are free from any significant mistakes. Moreover, an almost 5% error may have its source in possible experimental measurement inaccuracies.

In fact, the number of possible scenarios of a bird strike on the wing is infinite. Therefore, 12 representative test cases have been chosen for the purpose of the analysis. They have been grouped with respect to the following factors:

- Flight phase (impact velocity, incidence angle):
    a) Cruise (work) flight phase

    PZL-106 *Kruk* is meant to work at velocities between 160 and 200 km/h [22]. Therefore a mid-value, namely 180 km/h (50m/s) was chosen and additionally a bird velocity of 36 km/h (10m/s) in the opposite direction was added since this case has generally been intended to be more conservative. Using the lift equation, there is:

    $$L = \frac{1}{2}\rho_a V_{ac}^2 S C_L \tag{2}$$

    assuming steady level flight, i.e. $L = W_{ac}$, flight at sea level and knowing aircraft MTOW and wing area [22] we obtain:

    $$C_L = \frac{2W_{ac}}{\rho_a V_{ac}^2 S} = \frac{2*3500*9.81}{1.225*50^2*31.69} = 0.71 \tag{3}$$

    This value of lift coefficient for the aircraft of interest corresponds to 7^o angle of attack [22].

    b) Landing phase

    The landing stall velocity of the aircraft of interest is 80 km/h [22]. After implementation of a small safety margin the velocity of 25 m/s (90 km/h) has been chosen corresponding to the incidence angle of ca. 15^o. A bird velocity vector magnitude was assumed negligible compared to the one of an aircraft in this case.
- Mass of the bird
- Place of impact:: central impact, a rib impact and a bird hitting the slat leading edge close to the slat fixing on the left side of the component.

Table below presents all cases of analysis along with their parameters.

Table 2: The set of simulated cases

No	Title	Place of impact	Relative velocity [m/s]	Incidence angle [^{o}]	Bird mass [kg]
1	cent_land_0_5	Centre	25	15	0.5
2	cent_cruise_0_5	Centre	60	7	0.5
3	cent_land_1_8	Centre	25	15	1.8
4	cent_cruise_1_8	Centre	60	7	1.8
5	rib_land_0_5	Rib	25	15	0.5
6	rib_cruise_0_5	Rib	60	7	0.5
7	rib_land_1_8	Rib	25	15	1.8
8	rib_cruise_1_8	Rib	60	7	1.8
9	side_land_0_5	Side (fixing)	25	15	0.5
10	side_cruise_0_5	Side (fixing)	60	7	0.5
11	side_land_1_8	Side (fixing)	25	15	1.8
12	side_cruise_1_8	Side (fixing)	60	7	1.8

3 Results

The final mesh forms of all 12 analysed cases are shown below.

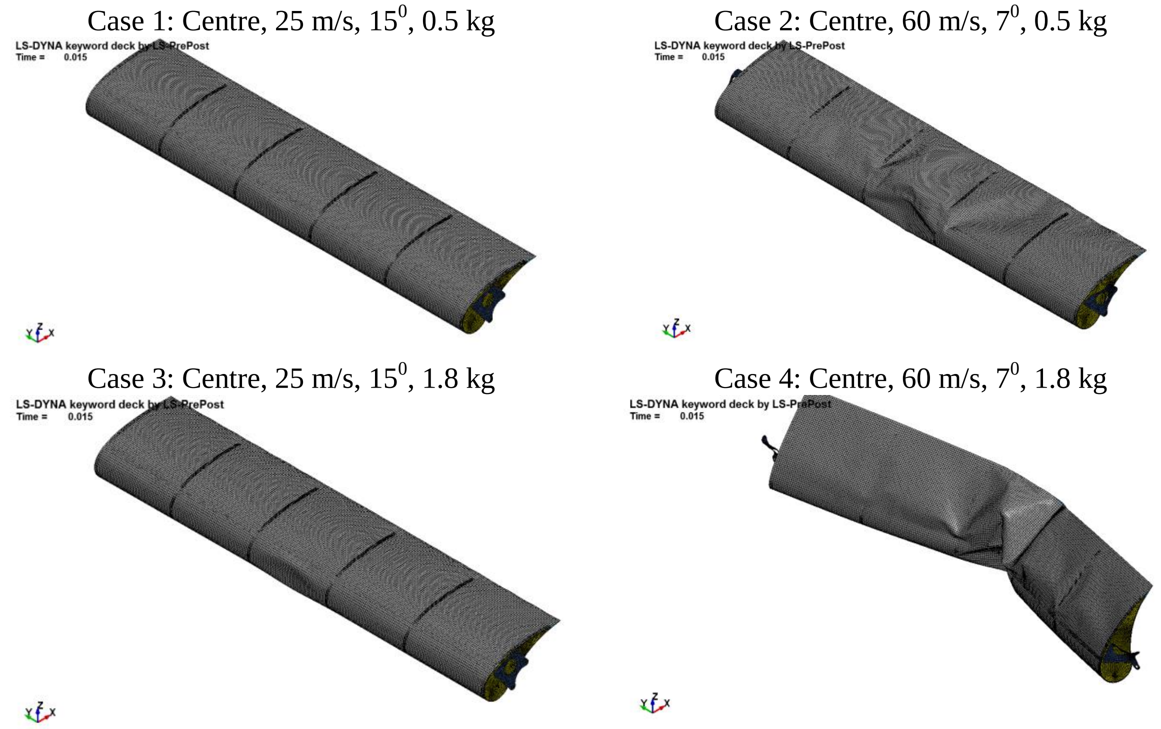

Figure 9: Final deformation for central impact cases

No permanent deformation occurs in case 1. The increase of a bird mass to 1.8 kg (case 3) results in a dent of 0.02 m depth between the middle ribs of the slat. The central impact at 60 m/s causes the deformation of the whole structure. A 0.5 kg bird causes the deformation of ca. 0.08 m mainly of the skin whereas the 1.8 kg bird impact damages the whole structure results in its detachment.

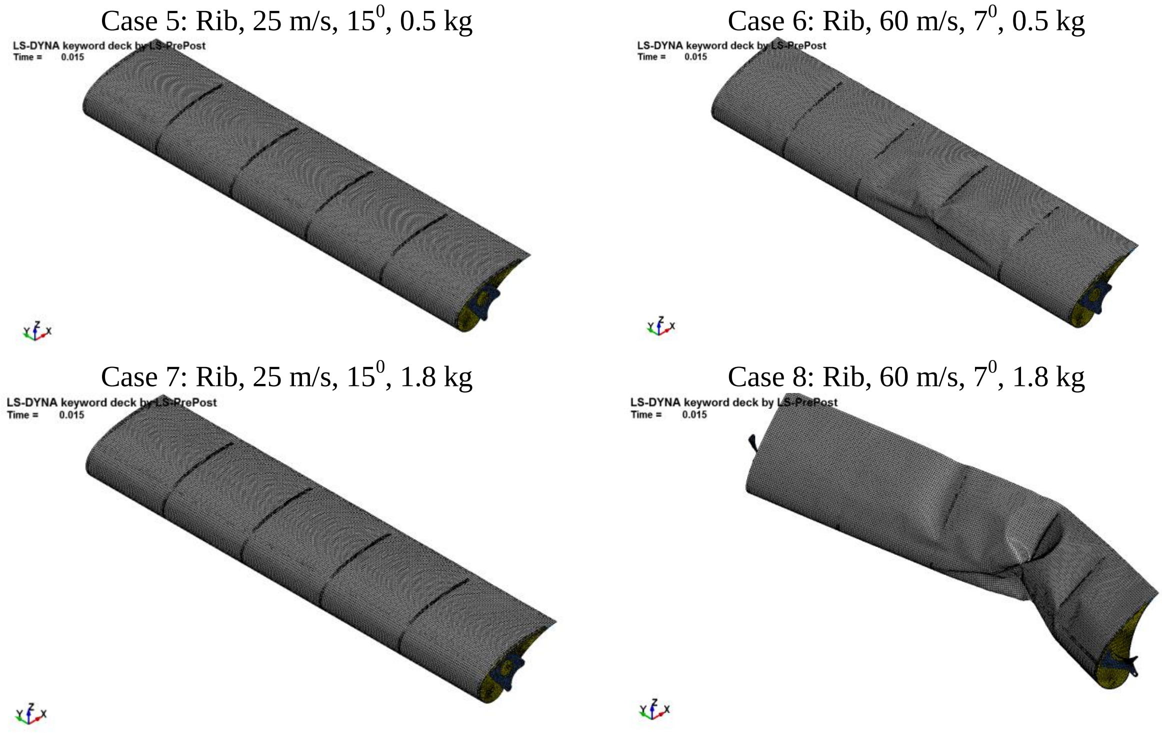

Figure 10: Final deformation for rib impact cases

A rib impact at 25 m/s causes no permanent deformation to the slat for both analysed bird masses. As the relative velocity reaches 60 m/s the 0.5 kg bird causes visible damage to the slat - the impacted nose rib collapses. The slat detaches after being hit by the 1.8 kg bird at 60 m/s.

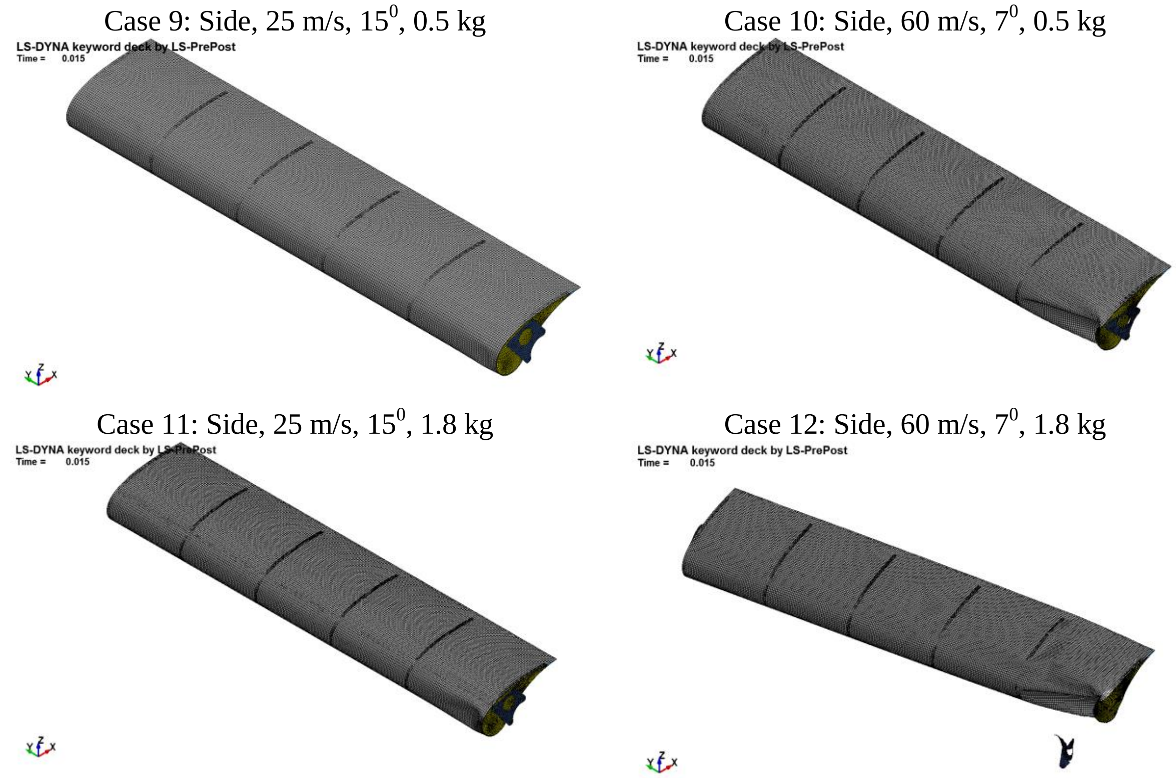

Figure 11: Final deformation for side impact cases

The impact of a 0.5 kg bird on the side of the slat at 25 m/s leaves a small dent of ca. 0.01 m depth. Both 0.5 kg bird at 60 m/s and 1.8 kg birds hitting the slat at the velocity of 25 m/s cause visible dents of depths 0.07 m and 0.025 m, respectively. A 1.8 kg bird strike causes almost immediate failure of the fixing and slat detachment.

A surface visualising the leading edge of the wing box has been generated and facilitated the determination of the wing box damage occurrence. An interference between the deformed slat shape obtained from calculations and the reference surface indicates that damage to the wing box might occur. The following figures show the comparison of the initial simulation state and heavily deformed slat resulting from case 4 calculation.

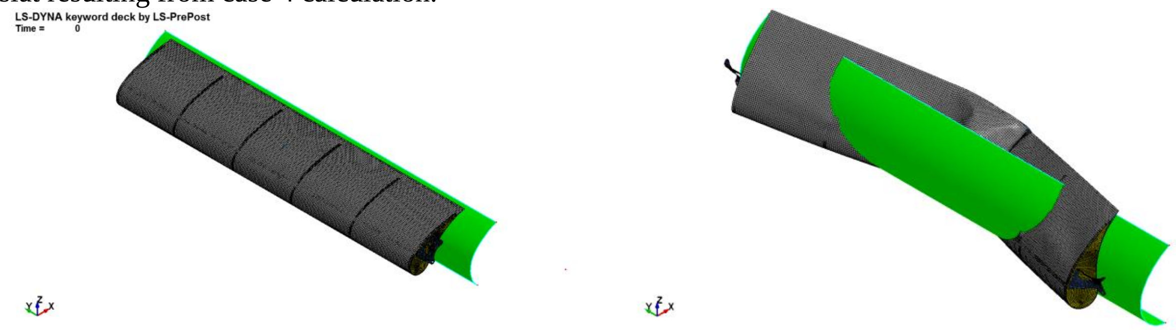

Figure 12: Leading edge slat and visualised wing box before and after the bird strike

Although the interference length between the slat and the surface visualising the wing box reaches 0.23 m the potential damage of the wing box is hard to estimate because of the fact that at the end of the simulation the part was still non-stationary. Nonetheless, a major damage to the wing box may be expected.

Another parameter registered during performed simulations were reaction force vectors at constrained nodes within the slat model. Figure 13 shows plots of the reaction force vectors magnitude for the simulation cases 1 and 4.

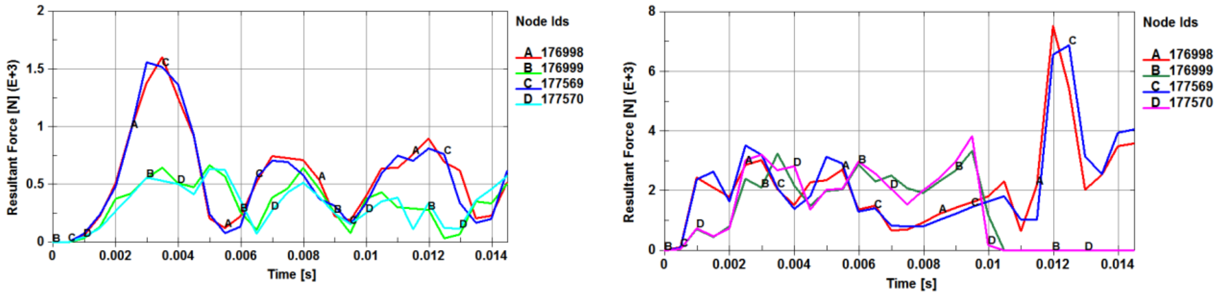

Figure 13: Case 1 (left) and 4 (right) resultant reaction vectors magnitude

The maximum reaction force encountered in the analysis at a single node is 7548 N. For the symmetric cases (Fig. 13) pairs of similar reaction forces may be observed. The magnitude of force appearing in the aft supports is generally higher than the one in the front supports. In case 4 both front support reactions drop to zero at time equal 10 milliseconds due to the failure of overstressed elements.

4 Discussion

The unforeseeable nature of the examined phenomenon makes obtained results rather qualitative than quantitative. However, presented results show a realistic prediction of the behaviour of analysed part in case of a bird impact.

In general, impacts of a bird with relative velocity of 25 m/s causes no or slight damage to the slat and poses no threat to the wing box, whatever the bird mass and place of contact are. When the relative velocity increases to 60 m/s mass of the bird plays a significant role, as the kinetic energy rises proportionally to the second power of the impact velocity. In this case 1.8 kg bird strike results in slat detachment no matter where it hits the part. It has been observed that all failures occurred in the slat fixing.

Since the slat is fixed to the wing by 4 bolts, failure of any of them could also possibly lead to slat detachment and, consequently, cause damage to the other wing parts. Taking it into account, reaction forces have been extracted. Analysed M6 bolts are made of 30HGSA steel of the tensile strength of 1080 MPa (110 kG/mm^3) according to the norm [23]. The shear strength has been estimated with the use of Tresca hypothesis to be equal $0.5s_{ut}$ which is a rather conservative approach [24]. Hence, given the bolt diameter D_b=6 mm one can calculate the maximum allowable reaction force R_{max} as follows:

$$R_{max} = s_{sh} * A_b = 0.5 * s_{ut} * \pi * (0.003)^2 = 15254\ N \qquad (4)$$

In the analysed cases obtained reaction forces did not exceed 8 kN, due to the preceding failure of an aluminium fixing. Therefore, this failure mode has been eliminated.

As shown in Figure 8 the structure was constrained by 4 SPC constraints which removed all but one degree of freedom from selected nodes. Slat segments are, however, arranged on a wing in sets of 4 next to each other. Therefore, 2 of them are limited from one side, the other from both. Figure 14 illustrates the highest displacement along y-axis of one of the aluminium fixing nodes. The peak value of Δ presented in the figure reaches 0.009 m for case 10. If neighbouring segments were taken into account this value could be close to zero due to additional reaction forces which could supposedly have an influence on final result. Therefore, a translational constraints along the y coordinate axis that act in one direction only should be considered. A way to achieve this may be to model a rigid wall next to the slat fixing. This method, however, may also induce some inaccuracies since neighbouring slat segments undoubtedly are not perfectly rigid.

The complete estimation of the consequences of a bird strike on the wing requires extending the research to the remaining part of the wing. Moreover, a parametric study over a wider range of velocities and bird masses can be performed aiming to identify the threshold of highly destructive conditions.

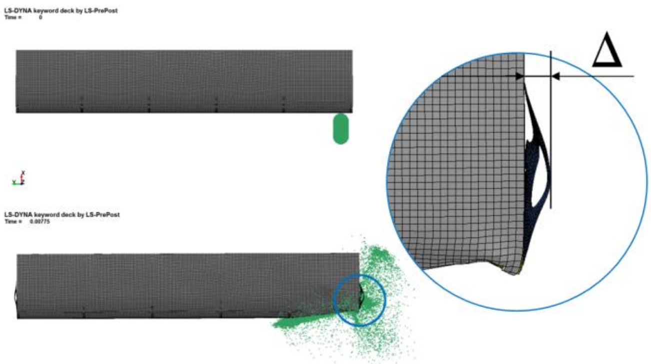

Figure 14: Transverse displacement of a slat fixing

In fact, performing such analyses requires researchers and manufacturers to own expensive commercial software licenses. Thus, an alternative method is widely used in engineering practise. It makes use of the static analysis and energy balance to examine dynamic problems according to the following chart:

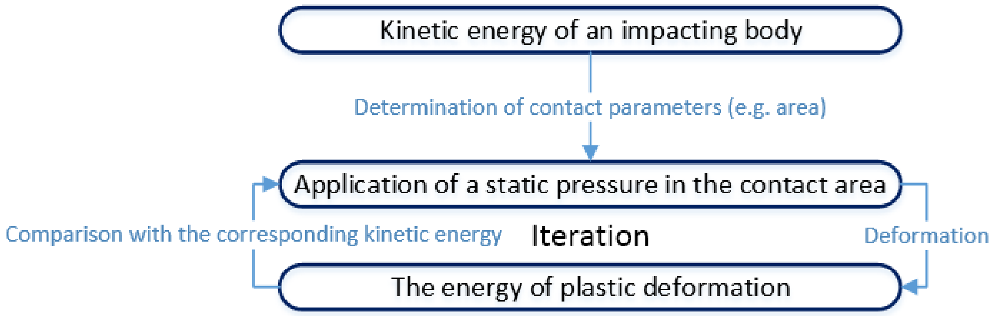

Figure 15: Alternative engineering method for impact problems

Further study will govern the comparison of both methods, development of a framework of performing a simplified analysis according to the presented procedure and will aim on defining necessary parameters (e.g. percentage of the kinetic energy transferred to plastic deformation energy).

5 Conclusions

A bird strike simulation on a slat segment of PZL-106 *Kruk* has been performed and the influence of various factors such as the impact velocity, angle of attack, bird mass and place of impact has been analysed. Slat damage for various scenarios has been estimated. The slat capability to protect the wing box from damage due to bird strike has been verified and conditions under which this capability is maintained have been indicated.

All objectives of the study have been fulfilled with the use of LS Dyna explicit finite element analysis software. The Smooth Particle Hydrodynamics formulation has been used in the finite element model of a bird. The validation of simulation results by the comparison with experimental data presented a good correlation. 12 different cases have been simulated and outcomes have been presented. The preliminary assessment of a wing box damage due to a bird strike has been performed with the use of a reference wing box surface. Limitations of the employed techniques have been explained and possible area for future research indicated. Results of this research provide information for the manufacturer about the behaviour of his product in case of a bird strike on a wing leading edge and show the potential of explicit finite element analysis in design and certification of small utility aircraft.

References

[1] Wright Brothers Aeroplane Company website: http://www.wright-brothers.org/ (accessed 28 July 2016)

[2] New York Times website: http://www.nytimes.com/topic/subject/us-airways-flight-1549 (accessed 28 July 2016)

[3] Bogusewicz P., Sala S.: Bird strike, czyli zderzenie z ptakiem, Warsaw, Prace Instytutu Lotnictwa, 2011

[4] Maragakis I.: Bird population trends and their impact on Aviation safety 1999-2008, European Aviation Safety Agency, 2009

[5] Shmotin Y.N., Chupin P.V., Romanov V.I.: Bird Strike Analysis of Aircraft Engine Fan, 7th European LS Dyna Conference, 2009

[6] Poola R.S.: Bird Strike Impact Analysis of Vertical Stabilizer Structure Using Abaqus/Explicit, SIMULIA India Regional Users Meeting, 2011

[7] Nagaraj V., Velmurugan T.: Numerical bird strike impact simulation of aircraft composite structure, IOSR Journal of Mechanical and Civil Engineering, ISSN: 2278-1684

[8] Guida M., Grimaldi A., Marulo F.: Bird impact on leading edge with SPH formulation, Composite Structures, 2011, ISSN: 0263-8223

[9] LS Dyna theory manual, Livemore Software

[10] National Aerospace Laboratory: Design and Testing of a Composite Birdstrike resistant leading edge, Technical Report, France, SAMPE Europe Conference, 2003

[11] Hedayati R., Sadighi M.: Bird Strike: An Experimental, Theoretical and Numerical Investigation, United Kingdom, 2016

[12] Daily Mail Online website: http://www.dailymail.co.uk/news/article-1180629 (accessed 28 July 2016)

[13] Czyż T.: LS Dyna: Wstęp do analiz dynamicznych, course materials, Warsaw, 2012

[14] ASM Aerospace Specification Metals website, http://aerospacemetals.com/ (accessed 28 July 2016)

[15] USA Department of Defence, Military Handbook: Metallic materials and elements for aerospace vehicle structures, USA, 1998

[16] Online Birds Catalogue, http://ptaki.info/index_siedliska.php?dzial=2&kat=10 &art=10, (accessed 28 July 2016)

[17] Federal Aviation Regulations, Part 25 Airworthiness Standards: Transport Category Airplanes

[18] McCallum S. C., Constantinou C.: The influence of bird shape in bird strike analysis, United Kingdom, 5th European LS Dyna Users Conference, 2005

[19] Australian Transport Safety Bureau: The Hazard Posed to Aircraft by Birds, Australia, 2002

[20] Walvekar V.: Bird strike analysis on leading edge of an aircraft wing using a Smooth Particle Hydrodynamics bird model, USA, Wichita State University, 2010

[21] Shen R. Wu, Lei Gu: Introduction to the explicit finite element method for nonlinear transient dynamics, USA, WILEY, 2012

[22] PZL "Warszawa – Okęcie" S.A.: PZL-106 Kruk design specification

[23] PN-72/H-84035 30HGS Steel Standard

[24] Pawlicki J.: Mechanics of Structures, lecture materials, Warsaw University of Technology, 2013